JOC The Journal of Organic Chemistry

Article

pubs.acs.org/joc

Tetraphenylethene-Based Star Shaped Porphyrins: Synthesis, Self-assembly, and Optical and Photophysical Study

Anushri Rananaware,[†] Rajesh S. Bhosale,[‡,∥] Kei Ohkubo,[§] Hemlata Patil,[†] Lathe A. Jones,[†,⊥] Sam L. Jackson,[†] Shunichi Fukuzumi,[§] Sidhanath V. Bhosale,[‡] and Sheshanath V. Bhosale*[,†]

[†]School of Applied Sciences, RMIT University, GPO Box 2476, Melbourne VIC-3001, Australia

[‡]Polymers and Functional Material Division, CSIR-Indian Institute of Chemical Technology, Hyderabad-500 007, Telangana India

[§]Department of Material and Life Science Graduate School of Engineering, Osaka University, GSE Common East 12F, 2-1 Yamada-oka, Suita, Osaka, 565-0871, Japan

[∥]RMIT-IICT Research Centre, CSIR-Indian Institute of Chemical Technology, Hyderabad-500 007, Telangana, India

[⊥]Centre for Advanced Materials and Industrial Chemistry (CAMIC), RMIT University, GPO Box 2476, Melbourne, Victoria 3001, Australia

Supporting Information

ABSTRACT: Supramolecular self-assembly and self-organization are simple and convenient ways to design and create controlled assemblies with organic molecules, and they have provoked great interest due to their potential applications in various fields, such as electronics, photonics, and light-energy conversion. Herein, we describe the synthesis of two π-conjugated porphyrin molecules bearing tetraphenylethene moieties with high fluorescence quantum yield. Photophysical and electrochemical studies were conducted to understand the physical and redox properties of these new materials, respectively. Furthermore, these derivatives were used to investigate self-assembly via the solvophobic effect. The self-assembled aggregation was performed in nonpolar and polar organic solvents and forms nanospheres and ring-like nanostructures, respectively. The solution based aggregation was studied by means of UV−vis absorption, emission, XRD, and DLS analyses. Self-assembled ring-shape structures were visualized by SEM and TEM imaging. This ring-shape morphology of nanosized macromolecules might be a good candidate for the creation of artificial light-harvesting nanodevices.

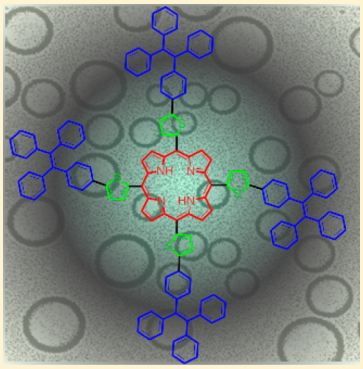

INTRODUCTION

Self-assembly and self-organization of optically active and planar aromatic molecules have generated much interest due to possible applications in versatile fields such as electronics, photonics, light-energy conversion, and catalysis.[1,2] Among aromatic molecules, porphyrin derivatives continue to attract much attention due to their unique π-conjugation and aggregation properties.[3,4] Porphyrinic derivatives have thus been used for the construction of molecular assemblies having well-defined shapes and dimensions, such as spheres, tubes, rods, nanosheets, nanorings, microrings, and nanowires.[5−10] Interesting morphologies that have been described include the self-assembly of structures from nanospheres to nanofibers, formation of nanosheets, and ring-shaped architectures.[11−16] Among all the above nanostructures, the ring-shaped assemblies of porphyrins are among those known to occur in nature, in the bacterial lightharvesting complex LH2.[17] In the LH2 complex, porphyrin molecules are arranged as in the ring of a turbine and are responsible for the absorption of light and storage and transportation of light energy to the reaction center, where it is converted into chemical energy. Photoinduced electron transfer (PET) and excited energy transfer (EET) reactions are essential processes for mimicking natural photosynthesis,[18,19] and these processes are very important for various applications, such as optoelectronic devices,[20] biological systems,[21] solar cells, and medicinal applications (photodynamic therapy).[22−24] In general, intramolecular PET and EET systems involve two chromophores, with porphyrins having received significant attention due to their similarity in structure to chlorophylls.[25,26]

On the other hand, mechanochromic luminescent materials have recently attracted attention due to their potential applicability in fields such as mechanosensors, security papers, and optoelectronic devices.[27,28] In 2001, the Tang group reported for the first time that luminescence of silole molecules is stronger in the aggregate state than in the solution state,[29,30] leading to the so-called "aggregation-induced emission" (AIE)[31] and "aggregation-induced emission enhancement" (AIEE)[32] phenomena. In recent years, tetraphenylethene (TPE) has become one of the best-known AIE fluorogens and its derivatives have found great potential in various applications such as chemosensors, bioprobes, solid-state emitters, as well as real-time cell apoptosis imaging.[33,34] Interestingly, TPE has also been used for supramolecular building blocks,[35−37] and

Received: January 13, 2015
Published: March 30, 2015

DOI: 10.1021/jo502760e
J. Org. Chem. 2015, 80, 3832−3840

Scheme 1. Synthesis of TPE-Porphyrin Derivatives 1 and 2

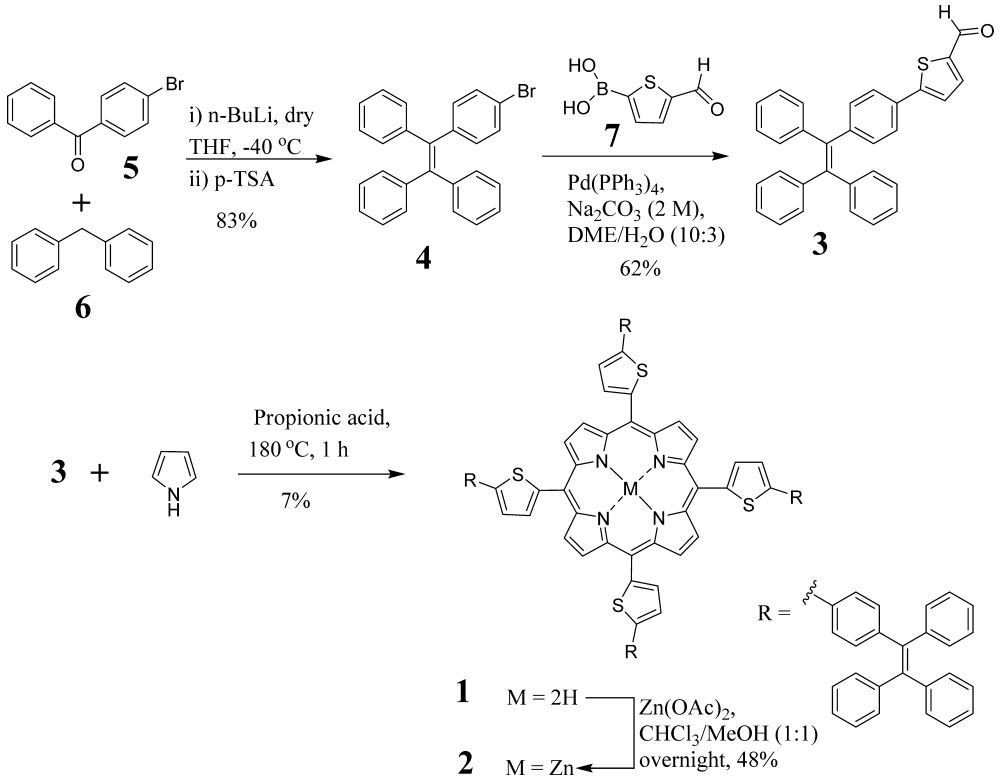

fluorescence "'turn on'" chemosensors for selective detection of Ag^{+} and Hg^{2+} ions.[34] In our previous work,[38] tetrapyridyl-based TPE was used for reversible sensing of H^{+}. Thus, continuing our efforts in the field, we are interested to develop materials with conjoint use of porphyrin and TPE moieities and to study their self-assembly and optical and photophysical properties.

RESULTS AND DISCUSSION

Synthesis. Herein, we report the synthesis of a new TPE-based porphyrin, its aggregation behavior via solvophobic control, and photophysical and electrochemical properties for the first time. The synthesis of TPE-porphyrins **1** and **2** is shown in Scheme 1. The synthesis started from the reaction of **5** with **6** in the presence of *n*-butyl lithium (*n*-BuLi, 2.5 M in hexane), followed by dehydration in the presence of *p*-toluene sulfonic acid (*p*-TSA), to afford bromo-TPE **4** in 83% yield. Suzuki coupling between **4** and (5-formylthiophen-2-yl)boronic acid (**7**) gave compound TPE-aldehyde **3** in 62% yield. TPE-porphyrin (**1**) was prepared by condensation of **3** with pyrrole in propionic acid at reflux temperature for 1 h, and gave 7% yield. Metallization of **1** with $Zn(OAc)_2$ in $CHCl_3$/MeOH gave zinc-TPE-por **2** in 48% yield.

UV–Vis Absorption and Fluorescence Spectroscopy. The TPE-por **1** and its zinc analogue **2** (ca. 1.2×10^{-4} M) are very soluble in chloroform and present a spectrum that is expected based on the porphyrinic core (Figure 1). The UV–vis absorption of **1** gives typical salient features including an intense Soret band at 447 nm ($\varepsilon = 3 \times 10^{5}$ M^{-1} cm^{-1}), along with four weaker Q-bands at 527, 578, 582, and 655 nm, and the band at 342 nm is a typical absorption band of TPE moieties.[19] Interestingly, all the bands in the absorption spectrum are largely red-shifted (see SI Figure S1) compared to 5,10,15,20-tetra(thiophen-2-yl)porphyrin (TThP).[39] The zinc analogue of TPE-por **2** (ca. 0.5×10^{-4} M) gives a sharp Soret band at 447 nm ($\varepsilon = 5 \times 10^{5}$ M^{-1} cm^{-1}) along with two typical Q-bands at 568 and 613 nm, and the band corresponding to TPE appeared at 337 nm. A range of concentrations were measured to ensure that a linear relationship was maintained between absorbance and emission intensities for both of the derivatives (**1** and **2**). These results show that the UV–vis absorption of the TPE-por derivatives can be readily tuned by the effect of TPE at the porphyrin core. The UV–vis absorption of the porphyrin derivatives is significantly red-shifted, which may be attributed to the elongated π-conjugation between the porphyrin and the four TPE moieties compared to zinc-TThP.[39]

The fluorescence spectra of **1** and **2** upon excitation at 440 nm in $CHCl_3$ solution are shown in Figure 1b. At this excitation wavelength, the porphyrin cores are selectively excited. As can be seen in Figure 1b, an intense emission band at about 700 nm was observed for **1** with a quantum yield of 15%, which is larger than that of free-base TThP (Figure S2, ~8%). This can be rationalized by the elogation π-conjugation between TPE and porphyrin moieties, which makes the molecule much more rigid and reduces the vibrational decay of the excited states efficiently. Similar fluorescence of the zinc analogue **2** (Figure 1b, blue line), excitation at 440 nm, results in emission from porphyrin at 650 nm with $\Phi_f = 0.12$, which is larger than that of ZnTPP ($\Phi_f = 0.010$).[39]

Solution Based Self-Assembly. We investigated the solvophobic effect on the aggregation behavior of TPE-Por **1**. Figure 2 shows the absorption spectra of **1** in a mixture of $CHCl_3$/MeOH and $CHCl_3$/cyclohexane. In the $CHCl_3$/cyclohexane mixture, it can be clearly seen that aggregation affects the spectrum with a significant blue-shift (5 nm) of the absorption band (iii) along with peak broadening. However, in $CHCl_3$/MeOH, the UV–vis absorption band (ii) is red-shifted (4 nm) with peak broadening. Fluorescence spectroscopy

DOI: 10.1021/jo502760e
J. Org. Chem. 2015, 80, 3832–3840

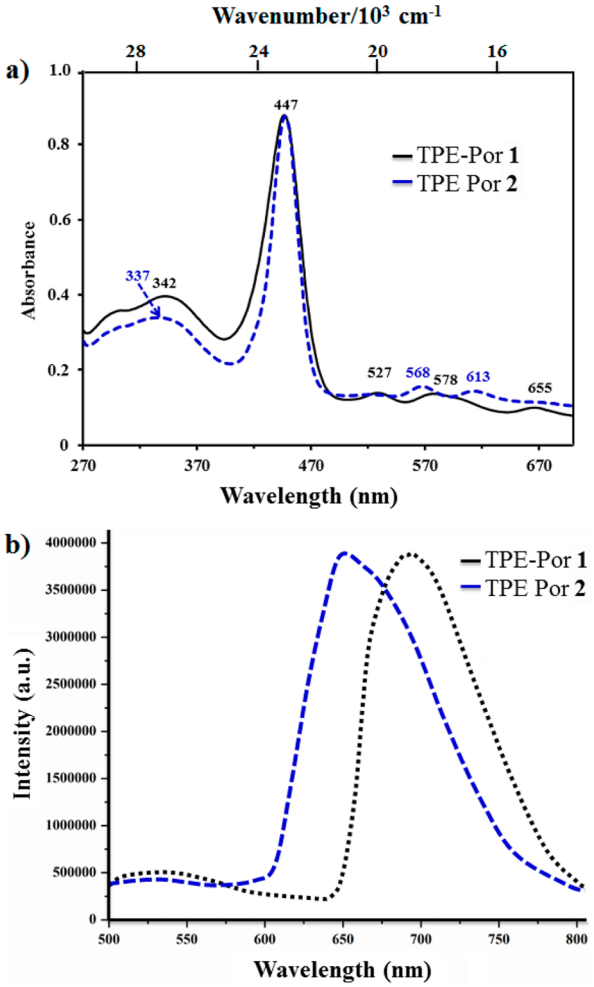

Figure 1. (a) UV−vis absorption and (b) emission spectra (λ_{ex} = 440 nm) of compounds **1** and **2** in $CHCl_3$, respectively.

provides evidence for aggregation of **1**, depending on the solvent used. Compound **1** shows emission at 700 nm in chloroform, which is blue-shifted (4 nm) in $CHCl_3$/cyclohexane (1:1, v/v). However, in $CHCl_3$/MeOH emission is decreased with peak broadening as shown in Figure 2b. This suggests that the mode of aggregation varies depending on the solvent used. Nevertheless, when more than 50% of MeOH or cyclohexane is used, the compound precipitates. The absorption and emission spectroscopy suggest the formation of face-to-face π-stacks of TPE-por chromophores similar to the ones reported in the case of J- and H-aggregates in other porphyrinic derivatives.[3−16]

Dynamic Light Scattering (DLS) Analysis of Nanostructures. To support the formation of nanostructures of **1** in $CHCl_3$/MeOH (1:1, v/v), the solution was assessed by dynamic light scattering (DLS) analysis. The extended assemblies with hydrodynamic diameters (D_H) of 20−100 nm were detected, besides larger assemblies of around 300−700 nm with the lapse of time (from top-to-bottom Figure 2c). Interestingly, the average D_H of assemblies showed a time-dependent increase that exceeded 0.5 μm after 30 min (3rd curve from bottom in Figure 2c). This is an indication of the presence of nonequilibrated, extended supramolecular assemblies that are expected to be spherical in shape. The combined results of UV−vis, emission, and DLS analysis suggest that there are different modes of aggregation depending on solvent used, which led us to further investigate the aggregation of **1** by means of scanning electron microscopy (SEM).

Scanning Electron Microscopy (SEM). Samples of **1** in 50% v/v cyclohexane or MeOH in $CHCl_3$ were spin coated onto silicon (111) wafers and analyzed by SEM. Compound **1** ([**1**] = 1 × 10^{-4} M) aggregated into well-formed ring-like nanostructures that extended down to nanometer sizes by changing the solvophobicity i.e. in 50% v/v $CHCl_3$/MeOH mixes (Figure 3a). Interestingly, three types of the ring-like nanostructures were identified. The sizes of the ring-like nanostructures are 0.25, 0.50, and 0.75 μm, indicating a doubling and then trebling of the thinnest of the porphyrin nanostructures. This is probably due to the fact that TPE-porphyrin **1** undergoes the nucleation process originated by 2-D coordination interactions with adjacent porphyrins which further comes together to form 3-D structures driven by the crystal lattice packing based on $\pi-\pi$ stacking of 2-D assembled layered structures during the self-assembly process. In the case of highly concentrated solutions of **1** (1 × 10^{-2} M), we observed the merging of a number of ring-like nanostructures into amorphous particles of porphyrins (see SI Figure S3−S5), while 1 × 10^{-6} M solution gave relatively small ring-like nanostructures which corresponded to the length of approximately one porphyrin molecule (see SI Figure S6).

In cyclohexane/$CHCl_3$ (50% v/v) mixture, compound **1** ([**1**] = 1 × 10^{-4} M) self-assembled into defined spherical aggregates that extended to nanometers in size, i.e. 150−300 nm (Figures 3b and S7). Compound **1** produced sheets at lower concentrations (10^{-6} M); however, at higher concentration (10^{-2} M), honeycomb-like morphologies were observed along with particles (see SI; Figure S8 and S9). It is important to mention that increasing the amount of MeOH or cyclohexane to beyond 50% causes the compound to precipitate out of the solution and no micro- or nanostructures were observed, which is an indication of the delicate balance of solvophobicity with noncovalent interactions that lead to nanostructure formation. No supramolecular structure is seen by this technique in pure chloroform.

An important factor to consider from a design point of view is that compound **2**, in which the porphyrin core is converted to the zinc analogue, failed to produce ring-like nanostructures, and only particular aggregates were observed at any proportion of MeOH or cyclohexane in $CHCl_3$ (See SI Figure S10).

Transmission Electron Microscopy (TEM). The ring-shaped nature of the supramolecule assembly of **1** was further confirmed by transmission electron microscopy (TEM) imaging. Figure 4 shows the TEM image of a droplete of $CHCl_3$/MeOH (1:1, v/v) of **1** (10^{-4} M) placed on a carbon-coated copper grid. Well-defined circular ring-shaped morphology is clearly seen with size varying in between 200 and 700 nm and the width of the rim at 10−25 nm, respectively (Figure 4a). To understand more about the effect of the solvents with self-assembly behavior, we changed the solvent and performed self-assembly in CH_3CN/MeOH and CH_3CN/cyclohexane. It can be clearly seen that **1** (10^{-4} M) in CH_3CN/MeOH (1:1, v/v) self-assembled into bundles of ring-shape morphology with size varying from 60 to 150 nm (Figure 4b). However, compound **1** in CH_3CN/cyclohexane (1:1, v/v) assembled into particular aggregates as shown in Figure 4c.

X-ray Powder Diffraction (XRD) Analysis. The nanostructure of **1** (10^{-4} M) was fabricated by injecting a small volume of solution of **1** ($CHCl_3$/MeOH, 1:1, v/v) into 1.5 mm diameter Lindéman capillaries and was characterized. The

DOI: 10.1021/jo502760e
J. Org. Chem. 2015, 80, 3832−3840

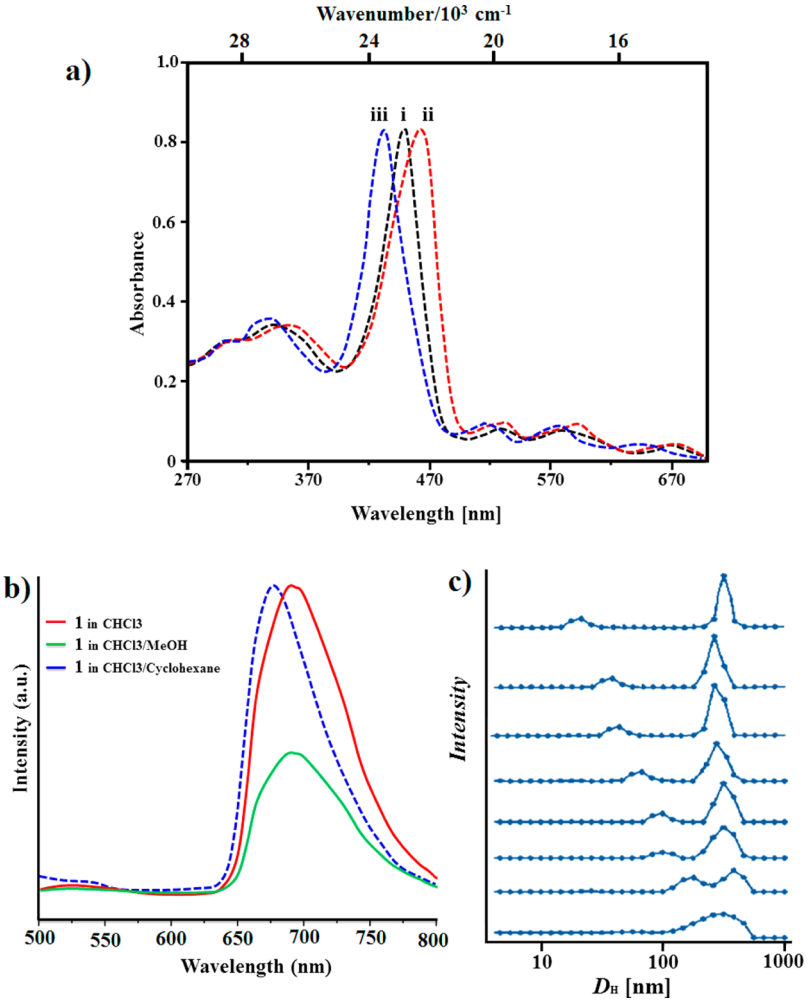

Figure 2. (a) UV−vis absorption and (b) fluorescence spectra (λ_{ex} = 378 nm) of compound **1** (1.0×10^{-4} M) in $CHCl_3$, $CHCl_3$/MeOH (1:1, v/v), and $CHCl_3$/cyclohexane (1:1, v/v), respectively. (c) Time-dependent (from top to bottom) changes of the hydrodynamic diameter (DH) distributions obtained by eight DLS measurements of solutions in $CHCl_3$/MeOH (1:1, v/v) of **1** (1×10^{-4} M). Data was started 10 min after the preparation of sample solutions and was taken at 5 min intervals.

internal structure of self-assembled aggregates was investigated by XRD analysis (Figure 4d). In the low angle range, the XRD diagram of the nanoscale hollow spheres formed from compound **1** in $CHCl_3$/MeOH shows typically three refraction peaks at 2θ = 1.83°, 2.41°, and 6.11°, corresponding to 5.10, 3.81, and 1.87 nm, respectively, which are ascribed to the refractions from the (010), (100), and (001) planes.[40]

The ring-sizes observed in TEM-, SEM-, and DLS-based assembly suggest a flattening upon being transferred from solution to the silicon surface. Although the self-assembly is predominantly driven by J- and H-type of aggregation via $\pi-\pi$-stacking interactions between the large aromatic cores of **1**,[41] solvophobicity plays an important role in the formation of each stack in ring-like nanostructures, as shown schematically in Figure 5. The formed assemblies are assumed to be the ring-shaped nanostructures observed by SEM and TEM and the similar sizes of the rings observed by DLS analysis.

Electrochemistry. Cyclic voltammetry was used to investigate the redox behavior of **1** and **2**. The free base TPE-porphyrin **1** shows two reversible reduction couples corresponding to formation of an anion radical and dianion, respectively, and an irreversible first oxidation couple for formation of a cation radical on the central porphyrinic π-ring system, which is preceded by an adsorption peak (Figure 6 and see Supporting Information for a data table and full details of electrochemical studies). The voltammogram for **2** shows that the introduction of Zn(II) affects the reversibility of the first radical anion under these conditions, with the first cathodic peak becoming irreversible followed by a quasireverisble couple. Comparing the first oxidation peak of **1** with the first oxidation peak of **2** (ignoring adsorption peaks), we see that there is not a significant shift due to the introduction of Zn(II), although the first reduction process of **2** does become easier, indicating stabilization of the LUMO orbital. If we use the onset potentials to estimate the electrochemical bandgap (E_g), the free ligand (**1**) is slightly larger, (1.74 V) compared to **2** (1.54 V).[42,43] The first oxidation peak of ZnTThP has been shown to have a $E_{1/2}$ value of 0.43 V, anodic of ZnTPP (0.34 V),[39] whereas **2** has a value of 0.39 V, indicating that the TPE groups make the porphyrinc core easier to oxidize compared to ZnTThP, due to the increased conjugation in the porphyrin ring.

Photophysical Study. Time-resolved transient absorption spectra of **1** were measured by femtosecond laser flash photolysis to study the dynamics of excited states. Transient absorption spectra observed after the femtosecond laser pulse

DOI: 10.1021/jo502760e
J. Org. Chem. 2015, 80, 3832−3840

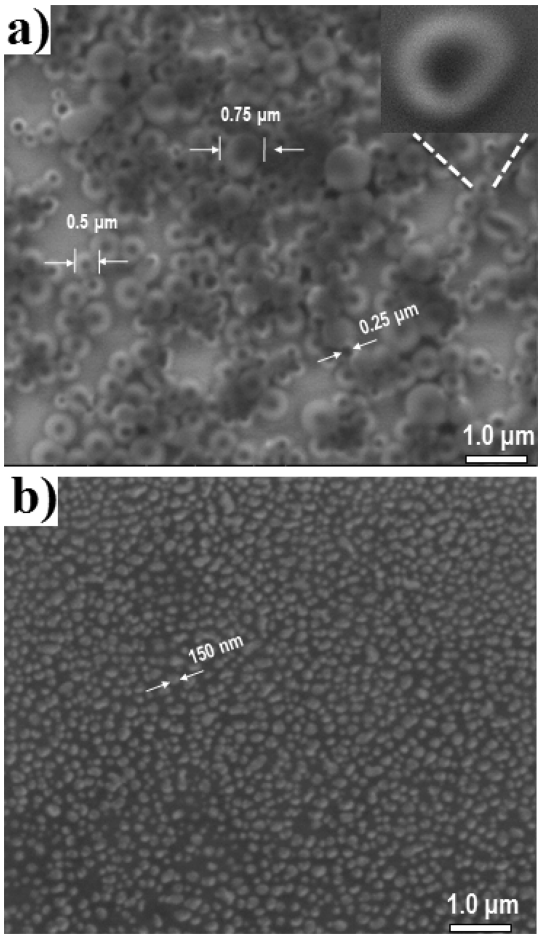

Figure 3. Scanning electron micrograph of **1** ([**1**] = 1 × 10^{-4} M) in (a) 50% v/v $CHCl_3$/MeOH and (b) 50% v/v $CHCl_3$/cyclohexane solvent mixtures, respectively. The bar represents 1 μm.

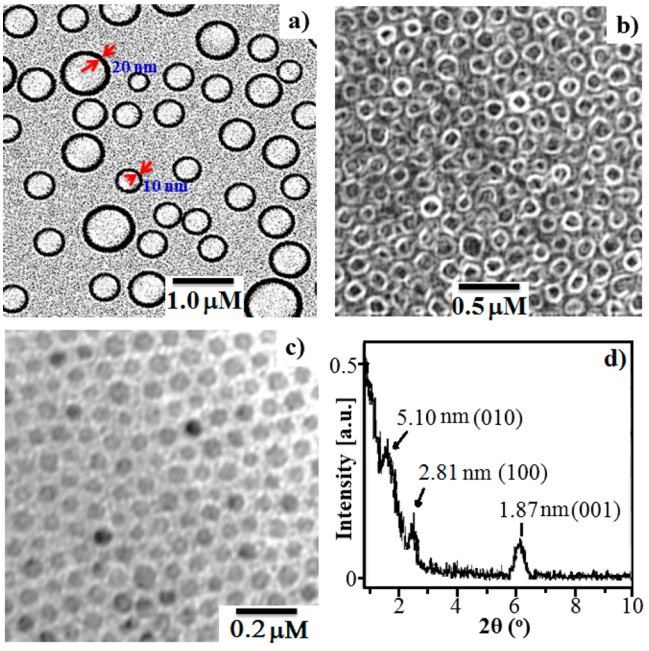

Figure 4. TEM images on a carbon-coated copper grid of **1** (10^{-4} M) from an equimolar mixture of (a) $CHCl_3$/MeOH, (b) CH_3CN/MeOH, and (c) CH_3CN/cyclohexane, respectively. (d) XRD profiles of the aggregates of compound **1** formed in $CHCl_3$/MeOH (1:1, *v*/*v*).

excitation at λ = 393 nm in a cyclohexane/CH_3CN (9:1, v/v) mix-solution of **1** are shown in Figure 7a. The transient absorption bands at 490, 550, 630, and 730 nm are those of the characteristic singlet excited state of **1**.[44] The intersystem crossing of the singlet excited state of **1** to the triplet was monitored at 730 nm (Figure 7b). The lifetime of the singlet excited state of **1** was determined as 1.4 ns, which is shorter than the excited state lifetime of the singlet excited states of a free base tetraphenylporphyrin (H_2TPP; τ = 10 ns)[45] and zinc tetrathienyl porphyrin (τ = 1.4 ns).[39] Thus, the intersystem crossing going to the triplet excited state is enhanced by the heavy atom effect of four sulfur nuclei in the thiophene spaces.[39] No electron transfer was observed between the porphyrin and tetraphenylethene entities. When the photodynamics of **1** were observed in the mix-solvent of MeOH/CH_3CN (9:1 v/v), the singlet excited state was significantly quenched with the lifetime of 1.4 ps (Figure 7b). This suggests that singlet−singlet annihilation to the S0 state occurs between π-stacked porphyrin molecules in a polar medium as show in Figure 4.[46] In the case of a zinc complex **2**, a similar behavior was observed as shown in Figure 7c and 7d.

X-ray Crystal Analysis. X-ray crystals of TPE-aldehyde **3** suitable for analysis were grown by vapor diffusion of hexane into a $CHCl_3$ solution (Figure 8).[47] The structure exhibits 2D packing with extensive $\pi-\pi$ interactions through the tetraphenylethene and thiophene. The layers have an alternating orientation of the molecules. Each phenyl ring of the tetraphenylethene has face-to-edge interactions with two other rings. Alternatively each thiophene exhibits face-to-face stacking with two other thiophenes in other layers (See Supporting Information Figure S10−S13). However, afterward several trial crystals of **1** and **2** were obtained by slow evaporation of a $CHCl_3$/cyclohexane mixture at room teperature. Unfortunately, the size of the crystals was too small to be analyzed by X-ray diffraction.

■ CONCLUSION

The results described herein are remarkable, as we demonstrate the possibility of constructing defined supramolecular architectures of ring-shaped morphology at micromolar concentrations of TPE-capped π-conjugated porphyrin molecules. The formation of rings was determined by SEM imaging, and photophysical studies support the π-stacking of TPE-porphyrins. Therefore, the present assembly is novel, as π-electronic segments are spatially arranged in closed circular ring-shape structures, which is reminiscent of the light-harvesting systems of purple photosynthetic bacteria in which the chlorophyll pigments are crucial for efficient excitation energy migration.[48] The electrochemical studies show that changes in the linker and the electronegativity of the substituents would be able to be tuned to control the band gap of the porphyrinic building block in supramolecular structures, which is especially important in applications involving electron transfer. We are also elaborating the current design strategy for the creation of various π-conjugated donor−acceptor functional architectures of defined size and shape.

■ EXPERIMENTAL SECTION

General Methods and Materials. All reagents were used as such without any further purification. All the solvents were received from commercial sources and purified by standard methods. Pyrrole, propionic acid, *p*-toluenesulfonic acid (PTSA), chloroform, methanol dichloromethane, and hexane were purchased and used without

DOI: 10.1021/jo502760e
J. Org. Chem. 2015, 80, 3832−3840

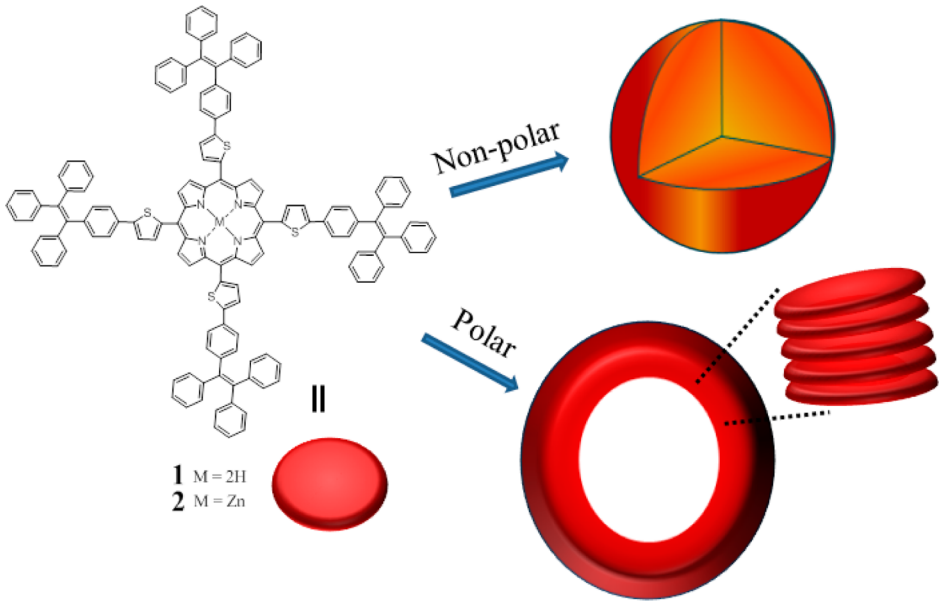

Figure 5. Graphical representation of self-assembled TPE-porphyrin in polar ($CHCl_3$/MeOH) and nonpolar ($CHCl_3$/cyclohexane) mixing solvent, respectively.

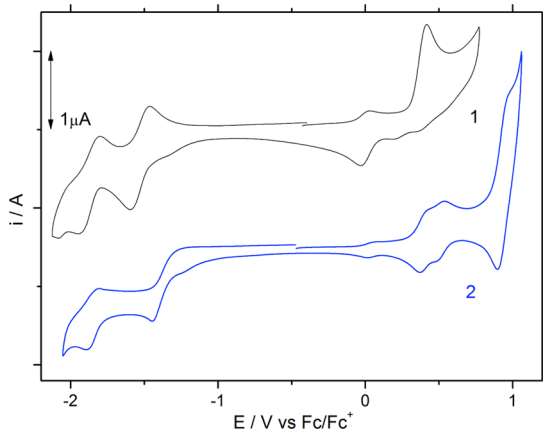

Figure 6. Cyclic voltammograms of **1** (black, top) and **2** (blue, bottom) in DCM/$TBAPF_6$ at a scan rate of 50 mV/s. Conditions: Glassy carbon working electrodes, Pt counter electrode, Ag pseudoreference electrode, and Fc/Fc^+ internal standard.

purification, unless otherwise specified. ^1H NMR and ^{13}C NMR spectra were recorded using chloroform-*d* as solvent and tetramethylsilane as an internal standard. The solvents for spectroscopic studies were of spectroscopic grade and used as received. Mass spectrometric data were obtained by the MALDI-TOF spectrometer technique.

Sample Preparation. Stock solutions ($c = 10^{-2}$ M) of **1** or **2** were made in $CHCl_3$. A 0.1 mL aliquot of the stock solution of each one was transferred separately to three different volumetric flasks of (i) $CHCl_3$ (100%), (ii) $CHCl_3$/MeOH (1:1, v/v), (iii) $CHCl_3$/MeOH (1:1, v/v) and made up to 2 mL volume with respective solvents. The solutions were allowed to equilibrate for 30 min prior to the UV–vis, flurescence spectroscopy, scanning electron microscopy (SEM), and transmission electron microscopy (TEM) measurements.

Fluorescence Spectroscopy. Fluorescence emission spectra were performed in a quartz cell with a 1 cm path length with 440 nm excitation wavelength.

Scanning Electron Microscopy (SEM). SEM measurements were performed on a FEI Nova NanoSEM operating at high vacuum, and SEM and images were collected. Freshly prepared 0.5 μL of TPE-porphyrin (**1** and **2**) samples were drop-cast on glass coverslips, and solvent was evaporated.

Transmission Electron Microscopy (TEM). A drop of solution of **1** (10^{-4} M) from respective solutions was cast onto a carbon copper grid, and the sample was allowed to stand for 20 s and removed of excess solution by blotting. The samples were then negatively stained with 5% (w/v) uranyl acetate for 5 min and allowed to dry, and images were measured on a JEOL-100CX II electron microscope operated at 80 kV.

Transient Absorption Spectroscopy. Femtosecond transient absorption spectroscopy experiments were conducted using an ultrafast source: Integra-C, an optical parametric amplifier: TOPAS, and a commercially available optical detection system: Helios provided by Ultrafast Systems LLC. The source for the pump and probe pulses was derived from the fundamental output of Integra-C (λ = 786 nm, 2 mJ/pulse and fwhm = 130 fs) at a repetition rate of 1 kHz. 75% of the fundamental output of the laser was introduced into a second harmonic generation (SHG) unit: Apollo (Ultrafast Systems) for excitation light generation at λ = 393 nm, while the rest of the output was used for white light generation. The laser pulse was focused on a sapphire plate of 3 mm thickness, and then a white light continuum covering the visible region from λ = 410 to 800 nm was generated via self-phase modulation. A variable neutral density filter, an optical aperture, and a pair of polarizers were inserted in the path in order to generate a stable white light continuum. Prior to generating the probe continuum, the laser pulse was fed to a delay line that provides an experimental time window of 3.2 ns with a maximum step resolution of 7 fs. In our experiments, a wavelength at λ = 393 nm of SHG output was irradiated at the sample cell with a spot size of 1 mm diameter, where it was merged with the white probe pulse in a close angle (<10°). The probe beam after passing through the 2 mm sample cell was focused on a fiber optic cable that was connected to a CMOS spectrograph for recording the time-resolved spectra (λ = 410–800 nm). Typically, 1500 excitation pulses were averaged for 3 s to obtain the transient spectrum at a set delay time. Kinetic traces at appropriate wavelengths were assembled from the time-resolved spectral data. All measurements were conducted at room temperature, 295 K.

Synthesis of 1-(4-Bromophenyl)-1,2,2-triphenylethene (4). This compound was prepared following a known literature procedure.[49] Typically, *n*-butyl-lithium (2.5 M in hexane, 19.0 mL, 47.59 mmol) was added dropwise to a solution of diphenylmethane **6** diphenylmethane (8.0 g, 47.59 mmol) in dry THF (350 mL) at 0 °C under nitrogen atmosphere. The resulting mixture was stirred for an

DOI: 10.1021/jo502760e
J. Org. Chem. 2015, 80, 3832–3840

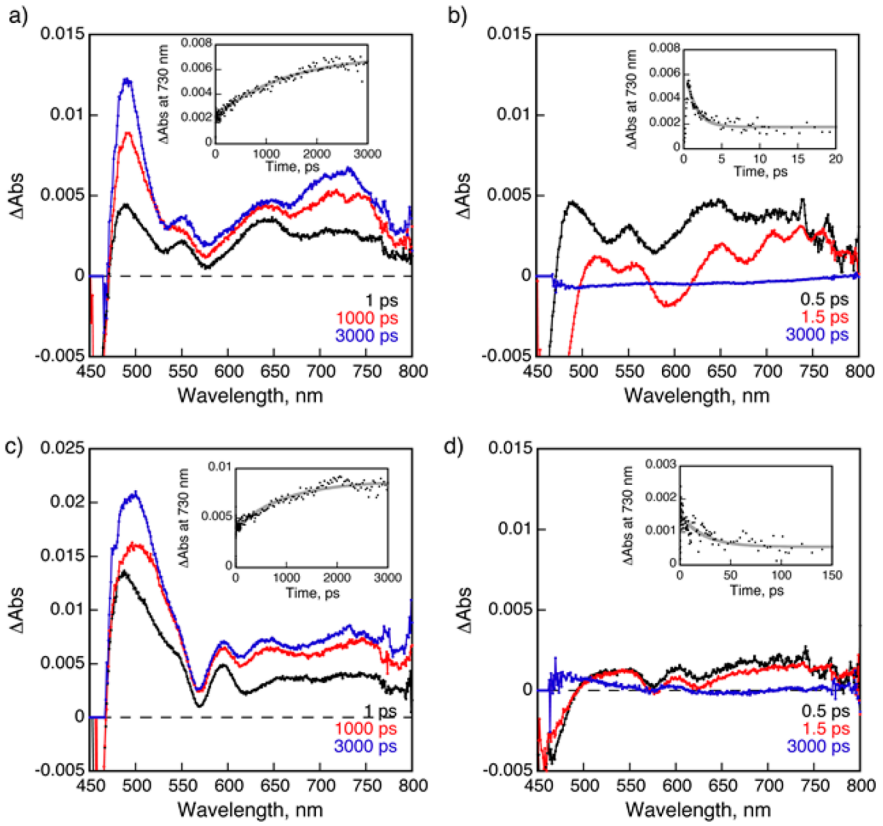

Figure 7. Transient absorption spectra of (a) **1** in cyclohexane/PhCN (9:1 *v*/*v*), (b) **1** in MeOH/PhCN (9:1 *v*/*v*), (c) **2** in cyclohexane/PhCN (9:1 v/v), and (d) **2** in MeOH/PhCN (9:1 v/v) taken after femtosecond laser excitation at 393 nm. Insets: Time profiles of absorbance at 730 nm. The gray lines were drawn by single-exponential curve fitting.

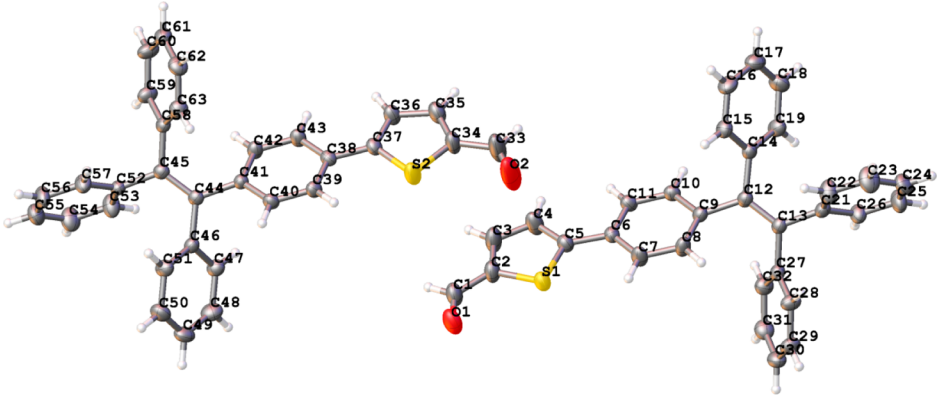

Figure 8. Ellipsoid representation of the asymmetric unit cell of intermediate compound **3** (hydrogen atoms omitted for clarity). Ellipsoids calculated at 50% probability.

additional 2 h at 0 °C. Then to it was added a solution of **5** (9.76 g, 37.59 mmol) in THF (60 mL), and the mixture was allowed to stir at room temperature for 10 h. Completion of the reaction was monitored by TLC analysis. After completion, the reaction mixture was quenched by adding aqueous solution of ammonium chloride, and then the mixture was extracted with DCM (3 × 50 mL). The organic layer was dried over anhydrous magnesium sulfate and evaporated via rotary evaporation to give a crude alcohol intermediate. This crude intermediate was then dissolved in toluene (100 mL), and *p*-toluenesulfonic acid (PTSA, 2 g) was added to it and refluxed for 16 h. After completion, reaction mixture was cooled to rt. Reaction mixture was evaporated via rotary evaporation to give crude residue which was purified by silica gel chromatography (40−60 nm) with *n*-hexane to give analytical pure compound **4** as white solid in 83% yield (16.3 g). All the data matches with reported compound **4**. ^{1}H NMR (300 MHz, $CDCl_3$) δ ppm: 7.27−7.21 (d, 2H, J = 6.0 Hz), 7.17−7.09 (m, 9H), 7.08−7.00 (m, 6H), 6.95−6.89 (d, 2H, J = 6.0 H_Z).

Synthesis of 5-(4-(1,2,2-Triphenylvinyl)phenyl)thiophene-2-carbaldehyde (3). Compound **4** (3.0 g, 7.30 mmol) was added to a solution of dimethyloxyethane (DME):2 M Na_2CO_3 (3:1, 100 mL) under argon atmosphere followed by addition of (5-formylthiophen-2-yl)boronic acid (1.48 g, 9.51 mmol), and the resulting reaction mixture was degassed for 15 min using argon. Then $Pd(PPh_3)_4$ (0.253 g, 0.21 mmol) was added, and the resultant mixture was heated to reflux at 150 °C for 24 h. Completion of the reactions was monitored by TLC analysis. After completion, reaction was quenched with water and extracted with DCM (3 × 75 mL). The combined organic layer was washed with water, dried over anhydrous sodium sulfate, and evaporated. Crude residue was purified by silica gel column chromatography, and the column was eluted with 5% MeOH in

DOI: 10.1021/jo502760e
J. Org. Chem. 2015, 80, 3832−3840

DCM, to give **3** as a yellow solid in 62% yield (2.0 g). ^{1}H NMR (300 MHz, $CDCl_3$) δ ppm: 9.8 (s, 1H), 7.62 (d, 1H, J = 3.9 Hz), 7.36−7.32 (d, 2H, J = 8.7 Hz), 7.26 (d, 1H, J = 4.2 Hz), 7.08−6.93 (m, 17H); ^{13}C NMR (75 MHz, $CDCl_3$) δ ppm: 182.7, 154.2, 145.3, 143.3, 143.2, 141.9, 149.9, 137.4, 132.1, 131.4, 131.3, 131.2, 127.9, 127.8, 127.6, 126.7, 126.6, 125.6, 123.8; Anal. Calcd for $C_{31}H_{22}OS$: C, 84.13; H, 5.01. Found: C, 84.14; H, 5.01.

Synthesis of 5,10,15,20-Tetrakis(5-(4-(1,2,2-triphenylvinyl)-phenyl)thiophen-2-yl)porphyrin (1). Condensation of **3** (1.0 g, 2.25 mmol) with equimolar amount of pyrrole (0.156 mL, 2.25 mmol) was heated in propionic acid (100 mL) at reflux temperature for 1 h. Thereafter, the resulting mixture was allowed to cool at 0 °C for 30 min. A black color solid residue was filtered through a Buchner funnel. The solid residue was washed with MeOH, and the crude residue was purified by silica gel column chromatography with 50% DCM in hexane to give pure compound as a blackish compound in 7% yield (0.3 g). ^{1}H NMR (300 MHz, $CDCl_3$) δ ppm: 9.09 (s, 2H), 7.75 (d, 1H, J = 3.6 Hz), 7.59 (d, 1H, J = 3.6 Hz), 7.57−7.51 (d, 2H, 8.4 Hz), 7.16−6.98 (m, 18H), −2.60 (bs, 2H); ^{13}C NMR (75 MHz, $CDCl_3$) δ ppm: 147.0, 143.7, 143.6, 141.7, 141.3, 140.4, 132.2, 132.1, 131.4, 131.3, 127.9, 127.7, 127.6, 126.6, 124.9, 122.0 Anal. Calcd for $C_{140}H_{94}N_4S_4$: C, 85.77; H, 4.83; N, 2.86. Found: C, 85.75; H, 4.81; N 2.84.

Synthesis of Zinc-5,10,15,20-tetrakis(5-(4-(1,2,2-triphenylvinyl)phenyl)thiophen-2-yl)porphyrin (2). To a stirred solution of TPE-porphyrin **1** (0.1 g, 0.051 mmol) in $CHCl_3$ (20 mL) was added a solution of $Zn(OAc)_2$ (0.1 g) in MeOH (2 mL), and the resultant mixture was allowed to stir at rt for 16 h. Reaction completion was checked by TLC analysis with spot disappearance of **1**. After completion, reaction mixture was evaporated on via rotary evaporator to complete dryness, and the crude residue obtained was purified by silica gel column chromatography. Compound **2** was eluted in 50% DCM in hexane as blackish solid in 48% yield (0.050 g). ^{1}H NMR (300 MHz, $CDCl_3$) δ ppm: 9.20 (s, 2H), 7.74 (d, 1H, J = 3.6 Hz), 7.60 (d, 1H, J = 3.6 Hz), 7.56 (d, 2H, J = 8.1 Hz), 7.16−6.98 (m, 19H); ^{13}C NMR (75 MHz, $CDCl_3$) δ ppm: 151.2, 143.7, 143.6, 143.4, 141.4, 132.1, 131.5, 131.4, 127.9, 127.7, 126.6, 124.9, 122.0; Anal. Calcd for $C_{140}H_{92}N_4S_4Zn$: C, 83.08; H, 4.58; N, 2.77. Found: C, 83.09; H, 4.59; N 2.79.

■ ASSOCIATED CONTENT

Ⓢ Supporting Information

SEM images of solvent dependent self-assembly, cyclic voltammograms, copies of NMR (^{1}H and ^{13}C), and Maldi spectra of compounds **1**, **2**, and **3**, and crystallographic data of **3**. Separate X-ray crystallographic data (CIF file). This material is available free of charge via the Internet at http://pubs.acs.org.

■ AUTHOR INFORMATION

Corresponding Author

*S.V.B.: fax: 0061399252680; Tel: 0061399252680; e-mail: sheshanath.bhosale@rmit.edu.au.

Notes

The authors declare no competing financial interest.

■ ACKNOWLEDGMENTS

S.V.B. (RMIT) acknowledges the Australian Research Council for financial support under a Future Fellowship Scheme (FT110100152) and the RMIT Microscopy and Microanalysis Facility (RMMF). S.V.B. (IICT) is grateful for financial support from the CSIR-Intel Coat (CSC 0114) and DST, New Delhi. L.A.J. acknowledges receipt of a Vice Chancellors (Industry) fellowship from RMIT University.

■ REFERENCES

(1) Whitesides, G. M.; Simanek, E. E.; Mathias, J. P.; Seto, C. T.; Chin, D. N.; Mammen, M.; Gordon, D. M. *Acc. Chem. Res.* **1995**, *28*, 37.
(2) Lehn, J.-M. *Angew. Chem., Int. Ed.* **1990**, *29*, 1304.
(3) Zuber, H.; Brunisholz, R. A. In *Chlorophylls*; Scheer, H., Ed.; CRC Press: Boca Raton, FL, 1991; pp 627.
(4) Jones, R.; Tredgold, R. H.; Hoorfar, A.; Hodge, P. *Thin Solid Films* **1984**, *113*, 115.
(5) Campidelli, S.; Sooambar, C.; Diz, E. L.; Ehli, C.; Guldi, D. M.; Prato, M. *J. Am. Chem. Soc.* **2006**, *128*, 12544.
(6) Imahori, H.; Fukuzumi, S. *Adv. Funct. Mater.* **2004**, *14*, 525.
(7) Nagata, N.; Kuramochi, Y.; Kobuke, Y. *J. Am. Chem. Soc.* **2009**, *131*, 10.
(8) Williams, F. J.; Vaughan, O. P. H.; Knox, K. J.; Bampos, N.; Lambert, R. M. *Chem. Commun.* **2004**, 1688.
(9) Bhosale, S. V.; Bhosale, S. V.; Kalyankar, M. B.; Langford, S. J.; Lalander, C. H. *Aus. J. Chem.* **2010**, *63*, 1326.
(10) Bhosale, S. V.; Chong, C.; Forsyth, C.; Langford, S. J.; Woodward, C. P. *Tetrahedron* **2008**, *64*, 8394.
(11) Bhosale, S. V.; Bissett, M. A.; Forsyth, C.; Langford, S. J.; Neville, S. M.; Shapter, J. G.; Weeks, L.; Woodward, C. P. *Org. Lett.* **2008**, *10*, 2943.
(12) Wang, Z. C.; Li, Z. Y.; Medforth, C. J.; Shelnutt, J. A. *J. Am. Chem. Soc.* **2007**, *129*, 2440.
(13) Lee, S. J.; Hupp, J. T.; Nguyen, S. T. *J. Am. Chem. Soc.* **2008**, *130*, 9632.
(14) Guo, P. P.; Chen, P. L.; Liu, M. H. *Langmuir* **2012**, *28*, 15482.
(15) Tretiak, S.; Middleton, C.; Chernyak, V.; Mukamel, S. *J. Phys. Chem. B* **2000**, *104*, 9540.
(16) Takazawa, K. *Chem. Mater.* **2007**, *19*, 5293.
(17) Schenning, A. P. H. J.; Benneker, F. B. G.; Geurts, H. P. M.; Liu, X. Y.; Nolte, R. J. M. *J. Am. Chem. Soc.* **1996**, *118*, 8549.
(18) McDermott, G.; Prince, S. M.; Freer, A. A.; Hawthormthwaite-Lawless, A. M.; Papiz, M. Z.; Cogdell, R. J.; Isaacs, N. W. *Nature* **1995**, *374*, 517.
(19) Guest, D.; Moore, T. A.; Moore, A. L. *Acc. Chem. Res.* **2009**, *42*, 1890.
(20) Aratani, N.; Kim, D.; Osuka, A. *Acc. Chem. Res.* **2009**, *42*, 1922.
(21) Albinsson, B.; Mårtensson, J. *J. Photochem. Photobiol. C: Photochem. Rev.* **2008**, *9*, 138.
(22) Senge, O. M.; Fazekas, M.; Notaras, E. G. A.; Blau, W. J.; Zawadzka, M.; Locos, O. B.; Mhuircheartaigh, E. M. *Adv. Mater.* **2007**, *19*, 2737.
(23) Herrero, C.; Lassalle-Kaiser, B.; Leibl, W.; Rutherford, A. W.; Aukauloo, A. *Coord. Chem. Rev.* **2008**, *252*, 456.
(24) Hiraku, Y.; Ito, K.; Hirakawa, K.; Kawanishi, S. *Photochem. Photobiol.* **2007**, *83*, 205−212.
(25) Giribabu, L.; Kanaparthi, R. K.; Velkannan, V. *Chem. Rec.* **2012**, *12*, 306.
(26) Yushchenko, O.; Hangarge, R. H.; Mosquera-Vazquez, S.; Bhosale, S. V.; Vauthey, E. *J. Phys. Chem. B* **2014**, DOI: 10.1021/jp5108685.
(27) Wasielewski, M. R. *Acc. Chem. Res.* **2009**, *42*, 1910.
(28) Davis, D. A.; Hamilton, A.; Yang, J. L.; Cremar, L. D.; Van Gough, D.; Potisek, S. L.; Ong, M. T.; Braun, P. V.; Martinez, T. J.; White, S. R.; Moore, J. S.; Sottos, N. R. *Nature* **2009**, *459*, 68.
(29) Kwon, M. S.; Gierschner, J.; Yoon, S. J.; Park, S. Y. *Adv. Mater.* **2012**, *24*, 5487.
(30) Li, Z.; Dong, Y. Q.; Lam, J. W. Y.; Sun, J. X.; Qin, A. J.; Haussler, M.; Dong, Y. P.; Sung, H. H. Y.; Williams, I. D.; Kwok, H. S.; Tang, B. Z. *Adv. Funct. Mater.* **2009**, *19*, 905.
(31) Wang, M.; Zhang, D. Q.; Zhang, G. X.; Zhu, D. B. *Chem. Commun.* **2008**, 4469.
(32) Luo, J.; Xie, Z.; Lam, J. W. Y.; Cheng, L.; Chen, H.; Qiu, C.; Kwok, H. S.; Zhan, X.; Liu, Y.; Zhu, D.; Tang, B. Z. *Chem. Commun.* **2001**, 1740.

DOI: 10.1021/jo502760e
J. Org. Chem. 2015, 80, 3832−3840

(33) Zeng, Q.; Li, Z.; Dong, Y.; Di, C. A.; Qin, A.; Hong, Y.; Ji, L.; Zhu, Z.; Jim, C. K. W.; Yu, G.; Li, Q.; Li, Z.; Liu, Y.; Qin, J.; Tang, B. Z. *Chem. Commun.* **2007**, 70.
(34) Tong, H.; Hong, Y.; Dong, Y.; Haussler, M.; Li, Z.; Lam, J. W. Y.; Dong, Y.; Sung, H. H. Y.; Williams, I. D.; Tang, B. Z. *J. Phys. Chem. B* **2007**, *111*, 11817.
(35) Shi, H.; Kwok, R. T. K.; Liu, J.; Xing, B.; Tang, B. Z.; Liu, B. *J. Am. Chem. Soc.* **2012**, *134*, 17972.
(36) Kapadia, P. P.; Widen, J. C.; Magnus, M. A.; Swenson, D. C.; Pigge, F. C. *Tetrahedron Lett.* **2011**, *52*, 2519.
(37) Zheng, Y.-R.; Zhao, Z.; Wang, M.; Ghosh, K.; Pollock, J. B.; Cook, T. R.; Stang, P. J. *J. Am. Chem. Soc.* **2010**, *132*, 16873.
(38) Rananaware, A.; Bhosale, R. S.; Patil, H.; Al Kobaisi, M.; Abraham, A.; Shukla, R.; Bhosale, S. V.; Bhosale, S. V. *RSC Adv.* **2014**, *4*, 59078.
(39) Rochford, J.; Botchway, S.; McGarvey, J. J.; Ronney, A. D.; Pryce, M. T. *J. Phys. Chem. A* **2008**, *112*, 11611.
(40) Minch, B. A.; Xiz, W.; Donley, C. L.; Hernandex, R. M.; Carter, C.; Carducci, M. D.; Dawson, A.; O'Brien, D. F.; Armstrong, R. R. *Chem. Mater.* **2005**, *17*, 1618.
(41) Kaiser, T. E.; Wang, H.; Stepanenko, V.; Würthner, F. *Angew. Chem., Int. Ed.* **2007**, *46*, 5541.
(42) Kadish, K. M.; Caemelbecke, E. V. *J. Solid State Electrochem.* **2003**, *7*, 254.
(43) Mussini, P. R.; Biroli, A. O.; Tessore, F.; Pizzotti, M.; Biaggi, C.; Carlo, G. D.; Lobello, M. G.; Angelis, F. D. *Electrochim. Acta* **2012**, *85*, 509.
(44) Ohkubo, K.; Sintic, P. J.; Tkachenko, N. V.; Lemmetyinen, H.; E, W.; Ou, Z.; Shao, J.; Kadish, K. M.; Crossley, M. J.; Fukuzumi, S. *Chem. Phys.* **2006**, *326*, 3.
(45) Horiuchi, H.; Tanaka, T.; Yoshimura, K.; Sato, K.; Kyushin, S.; Matsumoto, H.; Hiratsuka, H. *Chem. Lett.* **2006**, *35*, 662.
(46) Larsen, J.; Brüggemann, B.; Polívka, T.; Sundström, V.; Åkesson, E.; Sly, J.; Crossley, M. J. *J. Phys. Chem. A* **2005**, *109*, 10654.
(47) Crystal data for TPE-aldehyde **3**: $C_{31}H_{22}O_1S_1$, M = 442.55, 0.767 × 0.137 × 0.087 mm^3, monoclinic space group *P*21, a = 5.5812(7), b = 47.120(6), c = 9.2435(11) Å, α = 90, β = 103.343(3), Υ = 90, V = 2365.3(5), Z = 4, D_c = 1.243 g/cm^3, F_{000} = 928, T = 200(2) K, 1.73 < θ < 33.92°, 19180 reflection collected, 19180 unique (R_{int} = 0.0972), Final GoF = 1.028, *R*1 = 0.0659, *wR*2 = 0.1531, *R* indices based on 18751 reflections with $I > 2\sigma(I)$ (refinement on *F*2), 595 parameters.Crystallographic data for TPE-aldehyde **3** have been deposited with the Cambridge Crystallographic Data Centre as supplementary publication No. CCDC-1037259. Copies of the data can be obtained free of charge on application to CCDC, 12 Union Road, Cambridge CB21EZ, UK. Fax: (+44)1223-336-033; E-mail: deposit@ccdc.cam.ac.uk).
(48) Pullerits, T.; Sundström, V. *Acc. Chem. Res.* **1996**, *29*, 381.
(49) Banerjee, M.; Emond, S. J.; Lindeman, S. V.; Rathore, R. *J. Org. Chem.* **2007**, *72*, 8054.

DOI: 10.1021/jo502760e
J. Org. Chem. 2015, 80, 3832−3840